

# The Modelling of Biological Growth: a Pattern Theoretic Approach

Nataliya Portman, Postdoctoral fellow

McConnell Brain Imaging Centre  
Montreal Neurological Institute



McGill University



June 21, 2011

# Dedication

This research work is dedicated to my PhD co-supervisor

Dr. Ulf Grenander, the founder of Pattern Theory

Division of Applied Mathematics, Brown University

Providence, Rhode Island, USA.

<http://www.dam.brown.edu/ptg/>

# Outline

- 1 Mathematical foundations of computational anatomy
- 2 Growth models in computational anatomy
- 3 A link between anatomical models and the GRID model
- 4 GRID view of growth on a fine time scale
- 5 GRID equation of growth on a coarse time scale (macroscopic growth law)
- 6 Image inference of growth properties of the *Drosophila* wing disc
- 7 Summary, concluding remarks and future perspectives
- 8 Current work

# Mathematical foundations of computational anatomy

Computational anatomy<sup>1</sup> focuses on the precise study of the biological variability of brain anatomy.

D'Arcy Thompson laid out the vision of this discipline in his treatise “On Growth and Form”<sup>2</sup>. In 1917 he wrote

*“In a very large part of morphology, our essential task lies in the comparison of related forms rather than in the precise definition of each; and the deformation of a complicated figure may be a phenomenon easy of comprehension, though the figure itself may be left unanalyzed and undefined.”*

D'Arcy Thompson introduced the Method of Coordinates to accomplish the process of comparison.

---

<sup>1</sup> *Computational anatomy: An Emerging Discipline* by U. Grenander, M. I. Miller, *Quart. Appl. Math.*, **56(4)** 617-694 (1998)

<sup>2</sup> *On Growth and Form*, by D'Arcy Wentworth Thompson, Univeristy Press, 1917, 793 pages

# Mathematical foundations of computational anatomy

The Method of Coordinates reveals the phenomenon of correlation in regards to form within the family (e.g., primates).

Example: Evolution of the human skull shape<sup>3</sup>

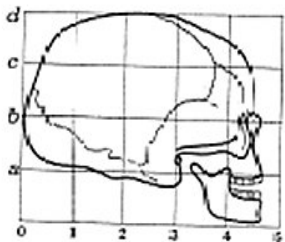


**Figure:** Human Skull

Skull of chimpanzee

Skull of baboon

<sup>3</sup> *On Growth and Form*, by D'Arcy Wentworth Thompson, Univeristy Press, 1917, 793 pages

# Mathematical foundations of computational anatomy

Thompson's vision has been cast into a precise mathematical form by Ulf Grenander and Michael Miller.

The anatomical configuration is a collection of 0,1,2,3-dimensional submanifolds with variabilities accommodated via random transformations (a [probabilistically deformable template](#)<sup>4</sup>).

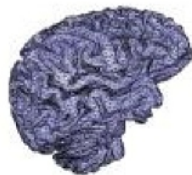
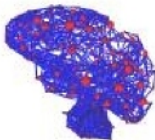
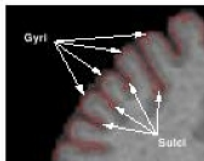


**Figure:** Gyri and sulci in a brain slice image, Sulcal landmarks and lines  
Triangulated graph of a brain surface

---

<sup>4</sup>*General Pattern Theory: A Mathematical Study of Regular Structures* by Ulf Grenander, Oxford University Press Inc., New York, NY, 1993

# Mathematical foundations of computational anatomy

Comparison of brain structures within a given anatomical population is achieved by means of **diffeomorphic transformations** (1-1 and onto, differentiable with differentiable inverse).

Importance of diffeomorphisms:

- Connected sets remain connected

# Mathematical foundations of computational anatomy

Comparison of brain structures within a given anatomical population is achieved by means of **diffeomorphic transformations** (1-1 and onto, differentiable with differentiable inverse).

Importance of diffeomorphisms:

- Connected sets remain connected
- Submanifolds such as surfaces are mapped as surfaces

# Mathematical foundations of computational anatomy

Comparison of brain structures within a given anatomical population is achieved by means of **diffeomorphic transformations** (1-1 and onto, differentiable with differentiable inverse).

Importance of diffeomorphisms:

- Connected sets remain connected
- Submanifolds such as surfaces are mapped as surfaces
- The global relationships between structures are preserved

# Mathematical foundations of computational anatomy

Comparison of brain structures within a given anatomical population is achieved by means of **diffeomorphic transformations** (1-1 and onto, differentiable with differentiable inverse).

## Importance of diffeomorphisms:

- Connected sets remain connected
- Submanifolds such as surfaces are mapped as surfaces
- The global relationships between structures are preserved
- The geometric features of individual anatomies (Gaussian curvature, Riemannian length, surface area) are maintained.

# Mathematical foundations of computational anatomy

Illustration of a large deformation diffeomorphic map.

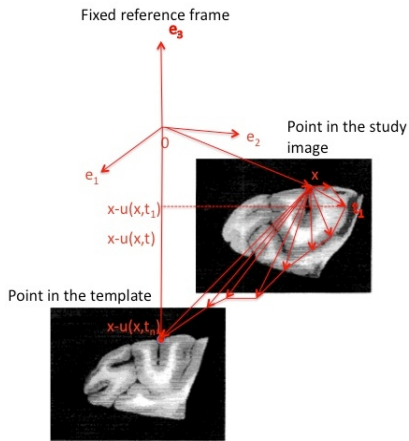


**Figure:** The monkey cortex cryosection,  $\mathcal{I}_{temp}$ , and the second monkey slice,  $\mathcal{I}$ .  $\vec{u}(x, t)$  is a time-dependent map  $\mathcal{I}_{temp}(x - \vec{u}(x, t)) \rightarrow \mathcal{I}(x)$ .

# Mathematical foundations of computational anatomy

## Diffeomorphic flows for large deformations are

- generated by continuum mechanics equations of motion

$$\vec{v} = \frac{d\vec{u}}{dt} = \frac{\partial\vec{u}}{\partial t} + \sum_{i=1}^d v_i \frac{\partial\vec{u}}{\partial x_i}$$

# Mathematical foundations of computational anatomy

## Diffeomorphic flows for large deformations are

- generated by continuum mechanics equations of motion

$$\vec{v} = \frac{d\vec{u}}{dt} = \frac{\partial \vec{u}}{\partial t} + \sum_{i=1}^d v_i \frac{\partial \vec{u}}{\partial x_i}$$

- constrained to the set of transformations consistent with the material properties of brain anatomy under study (elastic, visco-elastic, etc.)

$$\hat{v}(x, T) = \arg \min_{\vec{v}} E(\vec{v}(x, T), \vec{u}(x, T)) \quad (1)$$

$$= \arg \min_{\vec{v}} \{E_1(\vec{v}(x, T)) + E_2(\vec{u}(x, T))\}, \quad (2)$$

▶ more detail

# Mathematical foundations of computational anatomy

## Diffeomorphic flows for large deformations are

- generated by continuum mechanics equations of motion

$$\vec{v} = \frac{d\vec{u}}{dt} = \frac{\partial \vec{u}}{\partial t} + \sum_{i=1}^d v_i \frac{\partial \vec{u}}{\partial x_i}$$

- constrained to the set of transformations consistent with the material properties of brain anatomy under study (elastic, visco-elastic, etc.)

$$\hat{v}(x, T) = \arg \min_{\vec{v}} E(\vec{v}(x, T), \vec{u}(x, T)) \quad (1)$$

$$= \arg \min_{\vec{v}} \{E_1(\vec{v}(x, T)) + E_2(\vec{u}(x, T))\}, \quad (2)$$

▶ more detail

- $E_1(\vec{v}(x, T)) = \int_{[0, T]} \int_{\Omega} \|L(\vec{v}(x, t))\|^2 dx dt$ ,  $L$  is a differential operator from continuum mechanics,

# Mathematical foundations of computational anatomy

## Diffeomorphic flows for large deformations are

- generated by continuum mechanics equations of motion

$$\vec{v} = \frac{d\vec{u}}{dt} = \frac{\partial \vec{u}}{\partial t} + \sum_{i=1}^d v_i \frac{\partial \vec{u}}{\partial x_i}$$

- constrained to the set of transformations consistent with the material properties of brain anatomy under study (elastic, visco-elastic, etc.)

$$\hat{v}(x, T) = \arg \min_{\vec{v}} E(\vec{v}(x, T), \vec{u}(x, T)) \quad (1)$$

$$= \arg \min_{\vec{v}} \{E_1(\vec{v}(x, T)) + E_2(\vec{u}(x, T))\}, \quad (2)$$

▶ more detail

- $E_1(\vec{v}(x, T)) = \int_{[0, T]} \int_{\Omega} \|L(\vec{v}(x, t))\|^2 dx dt$ ,  $L$  is a differential operator from continuum mechanics,
- $E_2(\vec{v}(x, T)) = \frac{1}{2\sigma^2} \int_{[0, T]} \int_{\Omega} |\mathcal{I}_{temp}(x - \vec{u}(x, t)) - \mathcal{I}(x)|^2 dx dt$  is the observation energy needed to register template and study images.

# Bayesian view of transformations

- In Bayesian view, there exists a **prior probability density on a set of transformations**  $p(\vec{u})$ .

# Bayesian view of transformations

- In Bayesian view, there exists a **prior probability density on a set of transformations**  $p(\vec{u})$ .
- It is defined to give large probability to viscous fluid (elastic, visco-elastic) transformations.

# Bayesian view of transformations

- In Bayesian view, there exists a **prior probability density on a set of transformations**  $p(\vec{u})$ .
- It is defined to give large probability to viscous fluid (elastic, visco-elastic) transformations.
- Its exact form does not have to be specified.

# Bayesian view of transformations

- In Bayesian view, there exists a **prior probability density on a set of transformations**  $p(\vec{u})$ .
- It is defined to give large probability to viscous fluid (elastic, visco-elastic) transformations.
- Its exact form does not have to be specified.
- The solution  $\vec{u}(x, t), t \in [0, T]$  maximizes the posterior distribution  $p(\vec{u}|\mathcal{I})$  written in Gibbs form

$$p(\vec{u}|\mathcal{I}) \propto p(\mathcal{I}|\vec{u}) \cdot p(\vec{u}) \quad (3)$$

$$p(\mathcal{I}|\vec{u}) \cdot p(\vec{u}) = e^{-E(\vec{v}, \vec{u})} = e^{-(E_1(\vec{v}) + E_2(\vec{u}))}. \quad (4)$$

## Bayesian view of transformations

- In Bayesian view, there exists a **prior probability density on a set of transformations**  $p(\vec{u})$ .
- It is defined to give large probability to viscous fluid (elastic, visco-elastic) transformations.
- Its exact form does not have to be specified.
- The solution  $\vec{u}(x, t), t \in [0, T]$  maximizes the posterior distribution  $p(\vec{u}|\mathcal{I})$  written in Gibbs form

$$p(\vec{u}|\mathcal{I}) \propto p(\mathcal{I}|\vec{u}) \cdot p(\vec{u}) \quad (3)$$

$$p(\mathcal{I}|\vec{u}) \cdot p(\vec{u}) = e^{-E(\vec{v}, \vec{u})} = e^{-(E_1(\vec{v}) + E_2(\vec{u}))}. \quad (4)$$

- $E$  is the Gibbs potential, the sum of the prior energy  $E_1(\vec{v})$  and the Gaussian log-likelihood  $E_2(\vec{u})$ .

# Growth models in computational anatomy

- The equations of motion from mechanics have been used for computation of growth-induced shape changes seen in medical images.

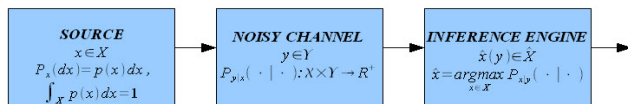
# Growth models in computational anatomy

- The equations of motion from mechanics have been used for computation of growth-induced shape changes seen in medical images.
- Bayesian interpretation of transformations provides a strong mathematical basis for image and landmark matching algorithms.

# Growth models in computational anatomy

- The equations of motion from mechanics have been used for computation of growth-induced shape changes seen in medical images.
- Bayesian interpretation of transformations provides a strong mathematical basis for image and landmark matching algorithms.
- The goal of these algorithms is to infer growth deformation fields determined by changes in pixel values.

# Growth models in computational anatomy



EXAMPLE IN COMPUTATIONAL ANATOMY

**DIFFEOMORPHIC  
MAPPING**  
 $\tilde{u}(x, t):$   
 $I_{template}(\tilde{x} - \tilde{u}(\tilde{x}, t)) \rightarrow I_{stud\phi}(\tilde{x})$

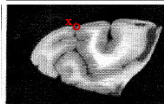
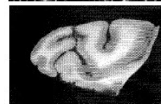
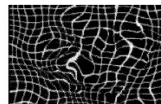


IMAGE PAIR

$(I_{template}(\tilde{x} - \tilde{u}(\tilde{x}, t)), I_{stud\phi}(\tilde{x}))$



INFERENCE RESULTS

$\hat{\tilde{u}}(\tilde{x}, T), \hat{I}_{stud\phi}$

**Figure:** The growth model in computational anatomy as Bayesian paradigm separating source from noisy observations.

(Images reproduced from *Deformable templates using large deformation kinematics* by R. D. Rabbitt, G. E. Christensen and M. I. Miller, IEEE Transactions on Image Processing, **5(10)** 1433-1447 (1996) )

# Growth models in computational anatomy

- Computational anatomy equations for growth generate very realistic structures.

# Growth models in computational anatomy

- Computational anatomy equations for growth generate very realistic structures.
- However, they do not reflect the underlying biology of shape change.

# A link between anatomical models and the GRID model

- From a biological perspective, it is not material constants that regulate growth, it is the [genetic control system](#).

# A link between anatomical models and the GRID model

- From a biological perspective, it is not material constants that regulate growth, it is the **genetic control system**.
- According to the book “**Endless forms most beautiful**” by S. B. Carroll, during growth a multicellular structure undergoes shape changes under the patterned control of a multitude of genes.

# A link between anatomical models and the GRID model

- From a biological perspective, it is not material constants that regulate growth, it is the **genetic control system**.
- According to the book “**Endless forms most beautiful**” by S. B. Carroll, during growth a multicellular structure undergoes shape changes under the patterned control of a multitude of genes.
- The genetic program of development unfolds in the form of spatial-temporal distribution of densities of gene products.

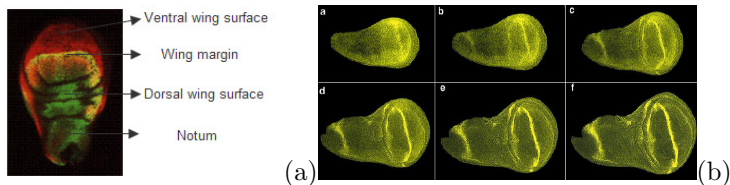


**Figure:** (a) Overlapping of the Vestigial and Apterous expression patterns, (b) Dynamics of the Wingless expression pattern during larval growth [ $\approx 48h$ ,  $\approx 120h$  after egg laying].

# A link between anatomical models and the GRID model

- From a biological perspective, it is not material constants that regulate growth, it is the **genetic control system**.
- According to the book “**Endless forms most beautiful**” by S. B. Carroll, during growth a multicellular structure undergoes shape changes under the patterned control of a multitude of genes.
- The genetic program of development unfolds in the form of spatial-temporal distribution of densities of gene products.

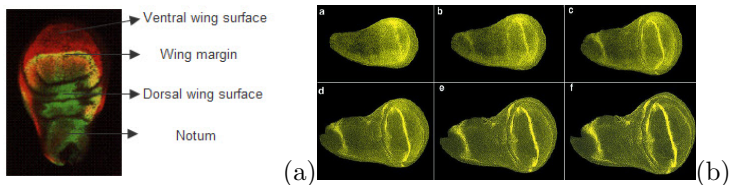


**Figure:** (a) Overlapping of the Vestigial and Apterous expression patterns, (b) Dynamics of the Wingless expression pattern during larval growth [ $\approx 48h$ ,  $\approx 120h$  after egg laying].

- At this level of small populations of cells a certain deformation is assigned.

# A link between anatomical models and the GRID model

The GRID model is **the first of its kind, genetically-based** mathematical model for a biological growth.

We are led to the dynamical model of growth as a sequence of genetically controlled transformations.

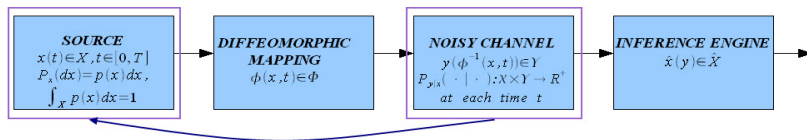


Figure: Schematic illustration of the GRID model.

We are looking for

- a smaller, more structured space  $\Phi$  of diffeomorphisms appropriate to modeling biological deformations,

# A link between anatomical models and the GRID model

The GRID model is **the first of its kind**, genetically-based mathematical model for a biological growth.

We are led to the dynamical model of growth as a sequence of genetically controlled transformations.

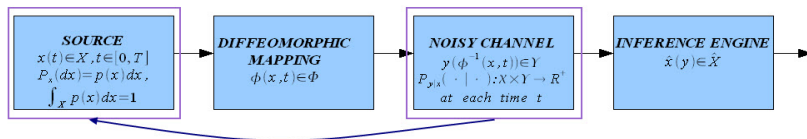


Figure: Schematic illustration of the GRID model.

We are looking for

- a smaller, more structured space  $\Phi$  of diffeomorphisms appropriate to modeling biological deformations,
- unknown structures hidden deeper in given observations of growth.

# GRID view of growth on a fine time scale

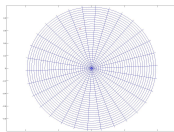
The **growth pattern** is a cumulative growth deformation composed of elementary deformations  $\phi^{(\xi_{seed}, t_i)}$

$$X(\xi, t_n) = \phi^{(\xi_{seed\sigma_n}, t_n)} \circ \phi^{(\xi_{seed\sigma_{n-1}}, t_{n-1})} \circ \dots \circ \phi^{(\xi_{seed\sigma_1}, t_1)} X(\xi, t_0).$$

# GRID view of growth on a fine time scale

Construction of the  $\phi$ -map:

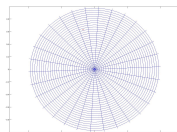
- Place a *seed* on a Darcyan grid according to a Poisson process.



# GRID view of growth on a fine time scale

Construction of the  $\phi$ -map:

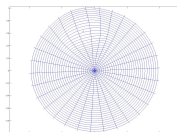
- Place a *seed* on a Darcyan grid according to a Poisson process.



- Deform the neighborhood around the seed

$\phi(x(\xi, t)) = x(\xi, t) + k(\tau)\mathcal{R}(x(\xi, t) - x(\xi_{seed}, t))$ , where

$$\mathcal{R}(\cdot) = (x(\xi, t) - x(\xi_{seed}, t)) \exp\left(-\frac{\|x(\xi, t) - x(\xi_{seed}, t)\|^2}{s^2}\right)$$

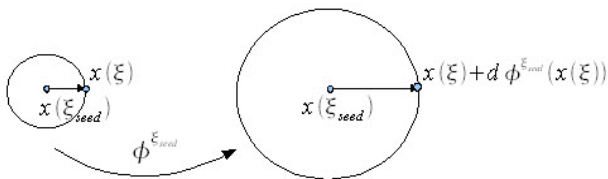


## Isotropic deformation patterns

$$\phi(x(\xi, t)) = x(\xi, t) + k(\tau)\mathcal{R}(x(\xi, t) - x(\xi_{seed}, t)).$$

If  $k(\tau) = \text{const}$  then the local deformation is **isotropic**.

The isotropic GRID transformation of a disk of radius  $s$  centered at the seed deforms it into a bigger or smaller disk.



# Isotropic deformation patterns

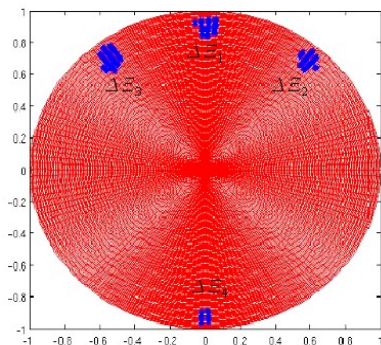


Figure: Isotropic locally expansive growth with active gene sets  $\bigcup_{i=1}^4 \Delta \Xi_i$ .

Click on an image to play a movie.

# Anisotropic deformation patterns

$$\phi(x(\xi, t)) = x(\xi, t) + k(\tau)\mathcal{R}(x(\xi, t) - x(\xi_{seed}, t)).$$

If  $k(\tau)$  is angle-dependent, then the deformation  $\phi^{\xi_{seed}, t}$  is anisotropic with one or more preferred directions of growth or decay.

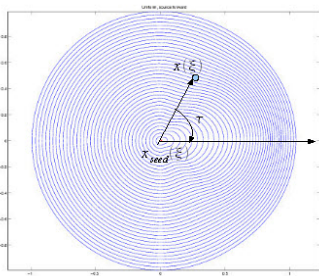
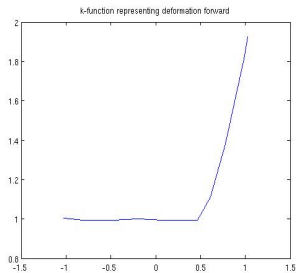


**Figure:** Angular deformation function  $k(\cos(\tau))$  and the corresponding deformation type “unipolar\_source\_forward”.

## Anisotropic deformation patterns

We specify gene activity region and build a growth pattern out of several elementary “uni-source-forward” maps.

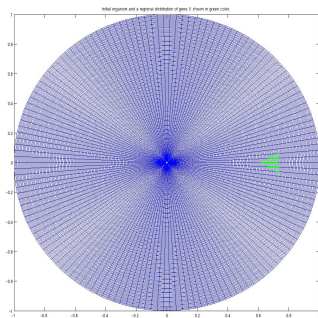


**Figure:** Gene activity region, unipolar source growth pattern and evolution of the Jacobian of the transformation with respect to the initially polar grid.

Click on an image to play a movie.

## Anisotropic deformation patterns

Similarly, we build a growth pattern out of several elementary “uni-sink-forward” maps.

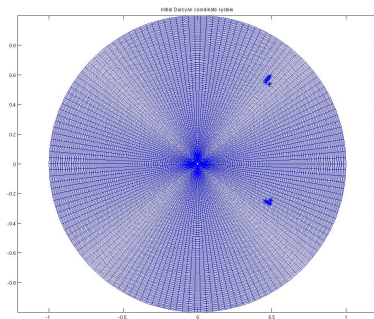


**Figure:** Gene activity regions, unipolar sink growth pattern and evolution of the Jacobian of the transformation with respect to the initially polar grid.

[Click on an image to play a movie.](#)

## Anisotropic deformation patterns

**Figure:** Two consecutive phases of chick wing development, “arm” and “forearm” with preferential directions of growth  $\tau = \pi/2$  and  $\tau = \pi/4$  correspondingly.

## Stochastic version of the isotropic GRID model

Imagine a growing organism as an evolution of a discrete particle configuration in absolute space-time driven by the inhomogeneous Poisson point process of seed activations.

Such a growth pattern  $\{x(\xi, t), t > t_0, \xi \in \Xi\}$  is a **Poisson-driven Markov process** described by the stochastic differential equation

$$dx = \int_{\xi_{t_j} \in \Xi} y^{\xi_{t_j}}(x) \mu(d\xi, dt) \text{ subject to } x(\xi, t_0) = x_0(\xi).$$

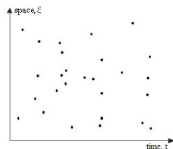


**Figure:** Spatial-temporal Poisson point process,  $\xi$ , spatial coordinate,  $t$ , time coordinate.

# Stochastic version of the isotropic GRID model

Experimental study of the Poisson-driven Markov process suggests the diffusive nature of interior seed paths.

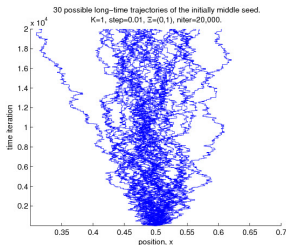


Figure: 30 realizations of 1D long-time Poisson-driven process.

## Stochastic version of the isotropic GRID model

We approximate the jump process by the diffusion process.

Namely, we derive the Fokker-Planck equation (FPE) describing the probability density of the 1D diffusive stochastic flow

$$\frac{\partial f(x, t)}{\partial t} = -\frac{\partial}{\partial x} (f(x, t) \cdot a(x)) + \frac{1}{2} \frac{\partial^2}{\partial x^2} (f(x, t) \cdot b(x))$$

with initial conditions  $f(x, t_0) = \sigma(x - \xi_0)$ .

## Stochastic version of the isotropic GRID model

We approximate the jump process by the diffusion process.

Namely, we derive the Fokker-Planck equation (FPE) describing the probability density of the 1D diffusive stochastic flow

$$\frac{\partial f(x, t)}{\partial t} = -\frac{\partial}{\partial x} (f(x, t) \cdot a(x)) + \frac{1}{2} \frac{\partial^2}{\partial x^2} (f(x, t) \cdot b(x))$$

with initial conditions  $f(x, t_0) = \sigma(x - \xi_0)$ .

FPE coefficients  $a(x)$  and  $b(x)$  reveal the space-dependent average velocity and the diffusion rate of the stochastic flow.

## Stochastic version of the isotropic GRID model

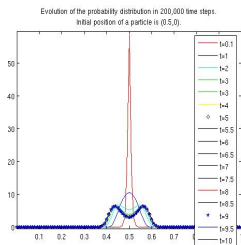
We approximate the jump process by the diffusion process.

Namely, we derive the Fokker-Planck equation (FPE) describing the probability density of the 1D diffusive stochastic flow

$$\frac{\partial f(x, t)}{\partial t} = -\frac{\partial}{\partial x} (f(x, t) \cdot a(x)) + \frac{1}{2} \frac{\partial^2}{\partial x^2} (f(x, t) \cdot b(x))$$

with initial conditions  $f(x, t_0) = \sigma(x - \xi_0)$ .

FPE time-dependent solutions reveal bimodal distribution of a random seed trajectory in space-time.



Evolution of the probability density  $f(x, t)$  of seed trajectories in time-space.

## Stochastic version of the isotropic GRID model

Future applications of the 2D Fokker-Planck equation include computation of macroscopic properties of the stochastic flow.

- Evolution of the mean seed trajectories in time.

$$\frac{d}{dt} \langle x(t) \rangle = \langle a(x(t)) \rangle .$$

- Evolution of the variance of seed trajectories in time.

$$\frac{d}{dt} \langle \langle x(t) \rangle \rangle = \langle b(x, t) \rangle + 2 \langle [x(t) - \langle x(t) \rangle] a(x(t)) \rangle$$

Maintaining the condition of independency of seed trajectories we can claim that these equations are meaningful macroscopic equations of growth on a fine time scale.

# GRID equation of growth on a coarse time scale

Motivation: A multitude of elementary biological events (cell divisions/deaths, enlargements and movements) results in visible shape and interior changes of a growing organism seen in images.



It seems natural to represent an underlying biological transformation by a diffeomorphic flow that evolves in time as a collective effect of a large number of cell decisions.

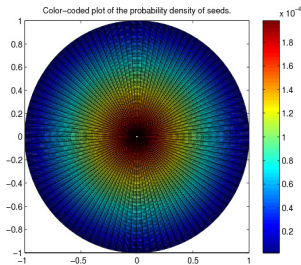


Figure: Macroscopic growth with space-dependent Poisson intensity.

## GRID equation of growth on a coarse time scale

The GRID equation of growth on a coarse time scale<sup>5</sup> is a continuum mechanics equation of motion with the velocity resulting from an infinite number of seed activations.

$$\frac{\partial x(\xi, t)}{\partial t} = \int_{\xi_{seed} \in \Xi} \Delta x^{\xi_{seed}}(\xi, t) \lambda(x(\xi_{seed}, t)) d\xi_{seed},$$

where  $\Delta x^{\xi_{seed}}(\xi, t)$  is an elementary deformation field due to a single seed placement at  $x(\xi_{seed})$   
 $\lambda(x(\xi_{seed}, t))$  is the Poisson intensity of seed placements.

---

<sup>5</sup>N. Portman, E.R. Vrscay, *Existence and Uniqueness of Solutions to the GRID Macroscopic Growth Equation*, Appl.Math. Comput. (2011), doi:10.1016/j.amc201.03.021, in press

## GRID equation of growth on a coarse time scale

The GRID equation of growth on a coarse time scale<sup>5</sup> is a continuum mechanics equation of motion with the velocity resulting from an infinite number of seed activations.

$$\frac{\partial x(\xi, t)}{\partial t} = \int_{\xi_{seed} \in \Xi} \Delta x^{\xi_{seed}}(\xi, t) \lambda(x(\xi_{seed}, t)) d\xi_{seed},$$

Growth is approximated by a diffeomorphic flow  $x(\xi, t)$  that depends on

- the Poisson intensity of seed placements  $\lambda(x(\xi_{seed}, t))$
- and the relative rate of expansion/contraction  $k(x(\xi, t))$  (the source).

We use the GRID macroscopic growth equation for image inference of the source of the diffeomorphic flow.

---

<sup>5</sup>N. Portman, E.R. Vrscay, *Existence and Uniqueness of Solutions to the GRID Macroscopic Growth Equation*, Appl.Math. Comput. (2011), doi:10.1016/j.amc201.03.021, in press

# Larval development of the *Drosophila* wing disc

**Biological facts** that have been taken into the 2D GRID model of the wing disc growth:

1. The observed dynamics of Wingless gene expression is tightly linked to the biological process of cell divisions.
2. Cells divide randomly and uniformly throughout the wing disc at larval stage of development.
3. Cell number doubles on average every 9 hours during the second and early third instar.
4. Most cell movements are due to passive displacements (newborn cells pushing extant ones).
5. The disc epithelium is one cell thick.

# Estimation of the intensity of cell decisions

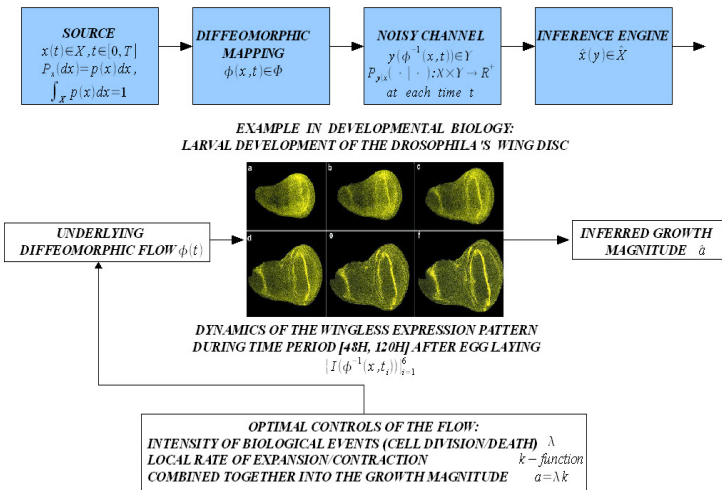


Figure: Inference of the GRID magnitude parameter from sensor data.

## Estimation of the intensity of cell decisions

The growth magnitude  $a(\xi_{seed}, t) = k(x(\xi_{seed}, t))\lambda(x(\xi_{seed}, t))$  is the unknown source of a biological deformation.

### Assumption.

- The absolute value of the local rate of expansion/contraction  $k(x(\xi_{seed}, t))$  is constant. It varies in sign throughout the cellular field.
- Let  $k(x(\xi_{seed}, t))$  be  $\pm 1$  and let  $\lambda$  absorb this constant for simplicity.
- The Poisson intensity of events in the Darcyan space is  $|\lambda(\xi_{seed}, t)|$ .

We would like to infer  $\lambda$ -field directly from image data.

## Estimation of the intensity of cell decisions

Using Bayes theorem we find a *maximum a posteriori* (MAP) estimate of  $\lambda(\xi, T)$

$$\arg \min_{\lambda \in R^N \times [0, T]} E_{post}(\lambda(\xi, T)) = \arg \min_{\lambda \in R^N \times [0, T]} [E_{likelihood}(\lambda(\xi, T)) + E_{prior}(|\lambda(\xi, T)|) + \Phi(\lambda(\xi, T))]$$

$E_{likelihood}(\cdot)$  relates observed pixel values with the growth parameter  $\lambda(\xi, T)$ ,

## Estimation of the intensity of cell decisions

Using Bayes theorem we find a *maximum a posteriori* (MAP) estimate of  $\lambda(\xi, T)$

$$\arg \min_{\lambda \in R^N \times [0, T]} E_{post}(\lambda(\xi, T)) = \arg \min_{\lambda \in R^N \times [0, T]} [E_{likelihood}(\lambda(\xi, T)) + E_{prior}(|\lambda(\xi, T)|) + \Phi(\lambda(\xi, T))]$$

$E_{prior}(\cdot)$  measures cell activities as represented by the Poisson intensity  $|\lambda(\xi, T)|$ ,

## Estimation of the intensity of cell decisions

Using Bayes theorem we find a *maximum a posteriori* (MAP) estimate of  $\lambda(\xi, T)$

$$\arg \min_{\lambda \in R^N \times [0, T]} E_{post}(\lambda(\xi, T)) = \arg \min_{\lambda \in R^N \times [0, T]} [E_{likelihood}(\lambda(\xi, T)) + E_{prior}(|\lambda(\xi, T)|) + \Phi(\lambda(\xi, T))]$$

$\Phi(\cdot)$  increases smoothness of  $\lambda(\xi, T)$  in the organism's domain.

$$\Phi(\lambda) = \|\nabla \lambda\|_2^2 = \int_{\xi \in \Xi} |\nabla \lambda(\xi, T)|^2 d\xi.$$

## Estimation of the intensity of cell decisions

Using Bayes theorem we find a *maximum a posteriori* (MAP) estimate of  $\lambda(\xi, T)$

$$\arg \min_{\lambda \in R^N \times [0, T]} E_{post}(\lambda(\xi, T)) = \arg \min_{\lambda \in R^N \times [0, T]} [E_{likelihood}(\lambda(\xi, T)) + E_{prior}(|\lambda(\xi, T)|) + \Phi(\lambda(\xi, T))]$$

subject to the discretized macroscopic growth equation

$$x(\xi, T) - x(\xi, 0) = \sum_{t=1}^T \sum_{\xi_{seed} \in \Xi} (x(\xi, t) - x(\xi_{seed}, t)) e^{\frac{-\|x(\xi, t) - x(\xi_{seed}, t)\|^2}{s(x(\xi_{seed}, t))^2}} \cdot \frac{1}{J(x(\xi_{seed}, (t-1)))} \lambda(\xi_{seed}, t)$$

with the initial conditions  $\lambda(\xi) = \frac{1}{N}$  ( $N$  is the total number of Darcyan seeds). This is the **optimal control problem** formulation.

# Prior models of the intensity field

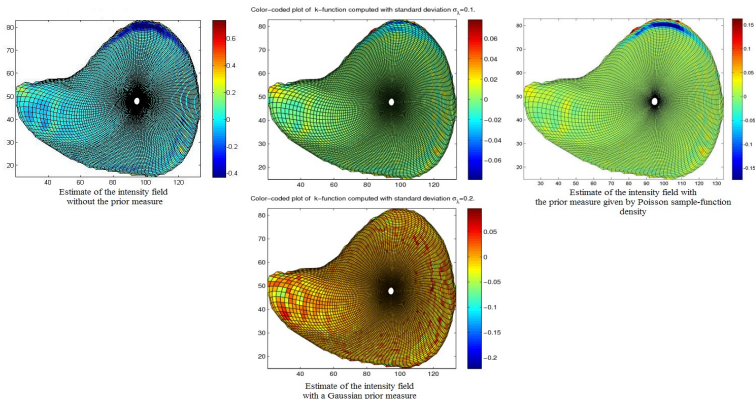
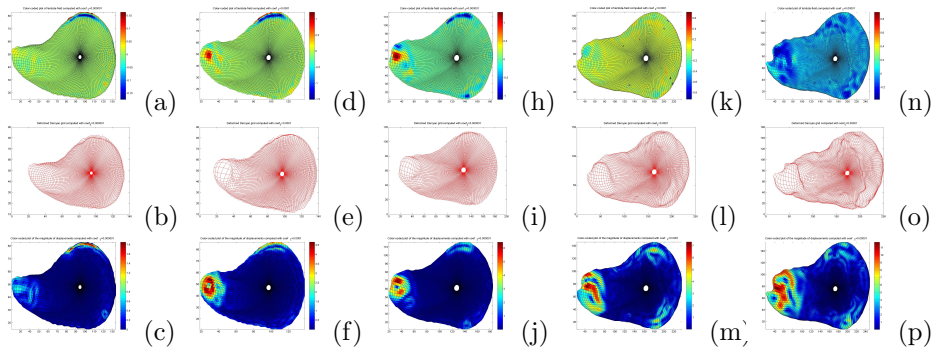


Figure: Left: no prior model,

middle: Gaussian prior  $E_{prior}(\lambda(\xi, t)) = \frac{1}{2\sigma_\lambda^2} \cdot \sum_{\xi \in \Xi} (\lambda(\xi, t) - \frac{1}{N})^2$ ,

right: Poisson prior  $E_{prior}(\lambda(\xi, t)) = - \sum_{[i=1]}^N \ln |\lambda(\xi_i, t)| + \sum_{[i=1]}^N |\lambda(\xi_i, t)|$

Inferred growth patterns of the *Drosophila* wing disc<sup>6</sup>.

**Figure:** Estimated  $\lambda(\xi)$  (top panel), deformed Darcyan grid of the wing disc generated by  $x(\xi, t)$  (middle panel) and magnitude of the displacements (bottom panel) for image pairs  $(I_1, I_2)$  (a-c),  $(I_2, I_3)$  (d-f),  $(I_3, I_4)$  (h-j),  $(I_4, I_5)$  (k-m),  $(I_5, I_6)$  (n-p).

<sup>6</sup>Portman N., Grenander U., Vrscay E., *GRID Macroscopic Growth Law and its Application to Image Inference*, Quarterly of Applied Mathematics, Vol. LXIX(2), 227–260 (2011)

# Hidden growth patterns of the *Drosophila* wing disc

**Figure:** The diffeomorphic flow  $x(\xi, t)$  of the Darcyan grid of the wing disc and the corresponding evolution of the pixel intensities  $I_1(x(\xi, t))$ .

Click on an image to play a movie.

# Summary

- 1 A pattern theoretic GRID model paves its way to the universal formal language of biological growth.

# Summary

- 1 A pattern theoretic GRID model paves its way to the universal formal language of biological growth.
- 2 The growth of biological shape is a digital stochastic process on the fine time scale and an analog deterministic process on the coarse time scale.

# Summary

- 1 A pattern theoretic GRID model paves its way to the universal formal language of biological growth.
- 2 The growth of biological shape is a digital stochastic process on the fine time scale and an analog deterministic process on the coarse time scale.
- 3 A systematic GRID-based approach for image analysis of growth has been developed into an algorithmic tool that automatically estimates growth characteristics of an organism directly from image data.

# Summary

- 1 A pattern theoretic GRID model paves its way to the universal formal language of biological growth.
- 2 The growth of biological shape is a digital stochastic process on the fine time scale and an analog deterministic process on the coarse time scale.
- 3 A systematic GRID-based approach for image analysis of growth has been developed into an algorithmic tool that automatically estimates growth characteristics of an organism directly from image data.
- 4 A biologically meaningful cost function in the form of the posterior probability is the most exciting result of this research.

# Summary

- 1 A pattern theoretic GRID model paves its way to the universal formal language of biological growth.
- 2 The growth of biological shape is a digital stochastic process on the fine time scale and an analog deterministic process on the coarse time scale.
- 3 A systematic GRID-based approach for image analysis of growth has been developed into an algorithmic tool that automatically estimates growth characteristics of an organism directly from image data.
- 4 A biologically meaningful cost function in the form of the posterior probability is the most exciting result of this research.
  - It measures not only the mismatch in images of initial and grown organisms but also cell activities driving observed shape changes.

# Summary

- 1 A pattern theoretic GRID model paves its way to the universal formal language of biological growth.
- 2 The growth of biological shape is a digital stochastic process on the fine time scale and an analog deterministic process on the coarse time scale.
- 3 A systematic GRID-based approach for image analysis of growth has been developed into an algorithmic tool that automatically estimates growth characteristics of an organism directly from image data.
- 4 A biologically meaningful cost function in the form of the posterior probability is the most exciting result of this research.
  - It measures not only the mismatch in images of initial and grown organisms but also cell activities driving observed shape changes.
  - It allows *maximum a posteriori* estimation of the intensity of elementary biological events underlying observed dynamics of levels of gene expression.

# Summary

- 1 A pattern theoretic GRID model paves its way to the universal formal language of biological growth.
  - 2 The growth of biological shape is a digital stochastic process on the fine time scale and an analog deterministic process on the coarse time scale.
  - 3 A systematic GRID-based approach for image analysis of growth has been developed into an algorithmic tool that automatically estimates growth characteristics of an organism directly from image data.
  - 4 A biologically meaningful cost function in the form of the posterior probability is the most exciting result of this research.
    - It measures not only the mismatch in images of initial and grown organisms but also cell activities driving observed shape changes.
    - It allows *maximum a posteriori* estimation of the intensity of elementary biological events underlying observed dynamics of levels of gene expression.
- The diffeomorphic flow corresponding to the optimal value of the  $\lambda$ -field does not fully register source and target images.

## Concluding remarks

This research has contributed to the development of

- a genetically-based model of a biological growth in quantitative biology,
- new computational methods in grid generation,
- optimization methods in image analysis,
- a new application of image analysis to the field of confocal microscopy.

## Future perspectives

The study of a link between gene expression patterns and generation of shape in a developing mouse brain.

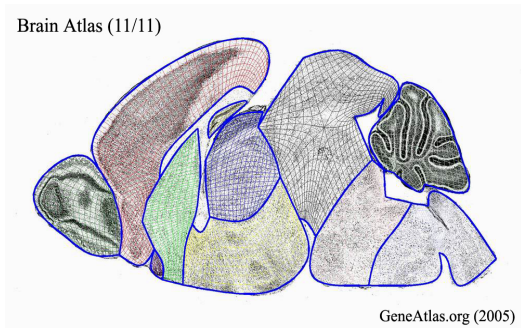


**Figure:** Brain atlas of a postnatal (day 7) mouse brain sagittal slice with the gene expression data (gene atlas) attached onto it. Cells expressing genes in anatomical subregions of the brain are stained in dark, [www. geneatlas. org ].

# Current work

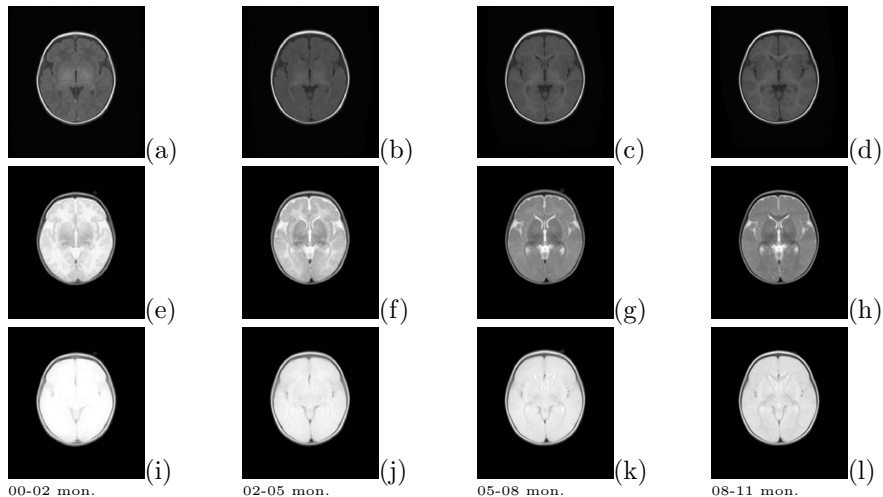


**Figure:** Axonal myelination during infant brain development affecting MRI signal. (a)-(d) T1-, (e)-(h) T2- and (i-l) proton density-weighted templates

## Current work

**Question: Which anatomical imaging modality should we rely on for the longitudinal study of early brain development?**

- Most longitudinal studies have been limited to T1-weighted images only.

## Current work

**Question: Which anatomical imaging modality should we rely on for the longitudinal study of early brain development?**

- Most longitudinal studies have been limited to T1-weighted images only.
- As a result, the automated image segmentation and cortical surface extraction procedures are hard to implement due to poor and highly variable grey/white matter contrast.

## Current work

**Question: Which anatomical imaging modality should we rely on for the longitudinal study of early brain development?**

- Most longitudinal studies have been limited to T1-weighted images only.
- As a result, the automated image segmentation and cortical surface extraction procedures are hard to implement due to poor and highly variable grey/white matter contrast.
- It is reasonable to combine information from all three MR anatomical images in the form of fused images with enhanced detail.

## Current work

**Question: Which anatomical imaging modality should we rely on for the longitudinal study of early brain development?**

- Most longitudinal studies have been limited to T1-weighted images only.
- As a result, the automated image segmentation and cortical surface extraction procedures are hard to implement due to poor and highly variable grey/white matter contrast.
- It is reasonable to combine information from all three MR anatomical images in the form of fused images with enhanced detail.
- This way uniqueness and fidelity of deformation fields induced by developmental process to all three types of MRI data can be established.

# Current work

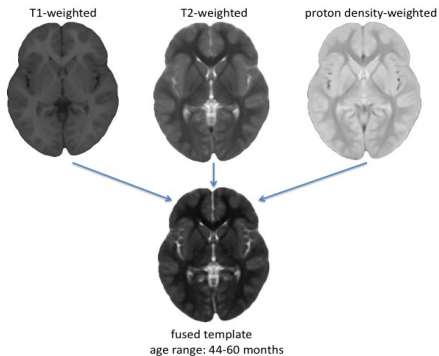


**Figure:** Fused template (44-60 mon.) obtained from T1-, T2- and PD-weighted templates <sup>7 8</sup> using wavelet-based approach.

---

<sup>7</sup> Alan C. Evans and Brain Development Cooperative Group, *The NIH MRI study of normal brain development*, NeuroImage 30 (2006), 184-202.

<sup>8</sup> V. Fonov, Ilana R. Leppert, B. Pike, D. L. Collins and the Brain Development cooperative Group, *MRI models of normal pediatric brain development from birth to 4.5 years: Part 1: Anatomical Templates* to be submitted to NeuroImage.

# Current work

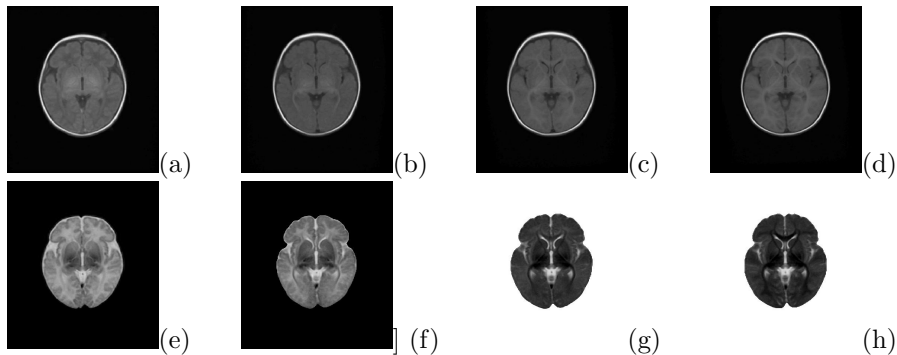
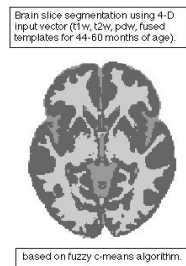
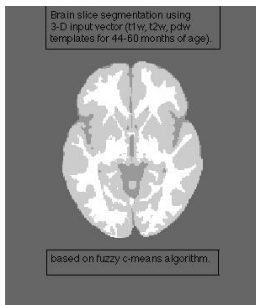


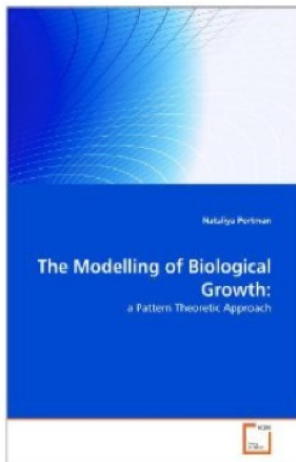
**Figure:** (a)-(d) T1-weighted atlas of normal early brain development and (e)-(h) its fused version.

# Current work

Adding a fused image to the existing three anatomical imaging modalities improves image segmentation.



# Literature



N. Portman, *The Modelling of Biological Growth: a Pattern Theoretic Approach*, VDM Verlag (May 2011), ISBN-10:3639303857, 304 pages, available at [www.amazon.ca](http://www.amazon.ca)

## Literature

- Portman N., Grenander U., Vrscay E., *New computational methods of construction of “Darcyan” biological coordinate systems*, Image Analysis and Recognition, Fourth International Conference ICIAR 2007 Proceedings, Vol.4633, August 2007, pp.143-156
- Portman N., Grenander U., Vrscay E., *Direct Estimation of Biological Growth Properties from Image Data Using the “GRID” Model*, Image Analysis and Recognition, Image Analysis and Recognition, Sixth International Conference ICIAR 2009 Proceedings, Vol.5627, pp.832-843
- Portman N., Grenander U., Vrscay E., *GRID Macroscopic Growth Law and its Application to Image Inference*, Quarterly of Applied Mathematics, Vol. LXIX(2), 227–260 (2011)
- Portman N., Vrscay E., *Existence and Uniqueness of Solutions to the GRID Macroscopic Growth Equation*, Appl. Math. Comput. (2011), doi:10.1016/j.amc.2011.03.021, in press, 11 pages.

# Literature

- [1] *The NIH MRI study of normal brain development*, by Alan C. Evans and Brain Development Cooperative Group, *NeuroImage* 30 (2006), 184-202.
- [2] *Automatic 3D Intersubject Registration of MR Volumetric Data in Standardized Talairach Space*, by D. L. Collins, P. Neelin, T. M. Peters and A. C. Evans, *Journal of Computer Assisted Tomography* 18(2) (1994), 192-205.
- [3] *Pipelines: Large scale automatic analysis of 3D brain data sets*, by A. Zijdenbos, A. Jimenez and A. Evans, 4th International Conference on Functional Mapping of the Human Brain, Montreal (1998), Organization for Human Brain Mapping, abstract no.783.
- [4] *3D statistical neuroanatomical models from 305 MRI volumes*, by A. C. Evans, D. L. Collins, S. R. Mills, E. D. Brown, R. L. Kelly and T. M. Peters, *Proc. IEEE-Nuclear Science Symposium and Medical Imaging conference* (1993), 1813-1817.
- [5] *Statistical Analysis of Cortical Surfaces*, by K. J. Worsley, D. MacDonald, J. Cao, K. Shafie, A. C. Evans, *NeuroImage* 3, S108.
- [6] *Unbiased Average Age-Appropriate Atlases for Pediatric Studies*, by V. Fonov, A. C. Evans, K. Botteron, C. R. Almlil, R. C. McKinstry, D. L. Collins and the Brain Development Cooperative Group, *NeuroImage* (2010), article in press.
- [7] *MRI models of normal pediatric brain development from birth to 4.5 years: Part 1: Anatomical Templates*, by V. Fonov, Ilana R. Leppert, B. Pike, D. L. Collins and the Brain Development cooperative Group, to be submitted to *NeuroImage*.
- [8] *Automated 3-D extraction and evaluation of the inner and outer cortical surfaces using a Laplacian map and partial volume effect classification*, by J. S. Kim, V. Singh, J. K. Lee, J. Lerch, Y. Ad-Dabbagh, D. MacDonald, et al. *NeuroImage* 27 (2005), 210-221.
- [9] *Anatomical Standardization of the Human Brain in Euclidean 3-space and on the Cortical 2-Manifold*, by S. M. Robbins, PhD thesis, School of computer Science, McGill University, Montreal, QC, Canada (2004).